The Journal of Immunology

Ligand Binding to Inhibitory Killer Cell Ig-Like Receptors Induce Colocalization with Src Homology Domain 2-Containing Protein Tyrosine Phosphatase 1 and Interruption of Ongoing Activation Signals

Yatin M. Vyas, Hina Maniar, Clay E. Lyddane, Michel Sadelain and Bo Dupont

J Immunol 2004; 173:1571-1578; ;
doi: 10.4049/jimmunol.173.3.1571
http://www.jimmunol.org/content/173/3/1571

The Journal of Immunology is published twice each month by
The American Association of Immunologists, Inc.,
1451 Rockville Pike, Suite 650, Rockville, MD 20852

Print ISSN: 0022-1767 Online ISSN: 1550-6606.

Ligand Binding to Inhibitory Killer Cell Ig-Like Receptors Induce Colocalization with Src Homology Domain 2-Containing Protein Tyrosine Phosphatase 1 and Interruption of Ongoing Activation Signals[1]

Yatin M. Vyas,[2]* Hina Maniar,[2†] Clay E. Lyddane,[†] Michel Sadelain,[†] and Bo Dupont[3†]

Interaction of NK cells with target cells leads to formation of an immunological synapse (IS) at the contact site. NK cells form two distinctly different IS, the inhibitory NK cell IS (NKIS) and the cytolytic NKIS. Cognate ligand binding is sufficient to induce clustering of inhibitory killer cell Ig-like receptors (KIR) and phosphorylation of both the receptor and the phosphatase Src homology domain 2-containing protein tyrosine phosphatase 1 (SHP-1). Recruitment and activation of SHP-1 by a signaling competent inhibitory receptor are essential early events for NK cell inhibition. We have in the present study used three-dimensional immunofluorescence microscopy to analyze distribution of inhibitory KIR, SHP-1, LFA-1, and lipid rafts within the NKIS during cytolytic and noncytolytic interactions. NK clones retrovirally transduced with the inhibitory KIR2DL3 gene fused to GFP demonstrate colocalization of KIR2DL3 with SHP-1 in the center of early inhibitory NKIS. Ligand binding translocates the receptor to the center of the IS where activation signals are accumulating and provides a docking site for SHP-1. SHP-1 and rafts cluster in the center of early inhibitory NKIS and late cytolytic NKIS, and whereas rafts continue to increase in size in cytolytic conjugates, they are rapidly dissolved in inhibitory conjugates. Furthermore, rafts are essential only for cytolytic, not for inhibitory, outcome. These results indicate that the outcome of NK cell-target cell interactions is dictated by early quantitative differences in cumulative activating and inhibitory signals. ***The Journal of Immunology*****, 2004, 173: 1571–1578.**

Natural killer cells recognize abnormal cells such as transformed tumor cells, virus-infected cells, and cells undergoing stress (1). Studies using tumor models have demonstrated that NK cells become activated upon interaction with target cells that have lost the expression of self MHC class I Ags, i.e., the missing self recognition (2). Malignant and virally transformed cells may, however, up-regulate ligands for the activating receptor NKG2D and over-ride inhibitory signals mediated by self-MHC (3–6). Alternatively, target cells may lose MHC class I expression and thereby induce NK activation (2). It is currently not known how concomitant inhibitory and activating signals are coordinated to regulate NK effector function.

The leukocyte receptor cluster on human chromosome 19q13.42 contains the killer cell Ig-like receptor (KIR)[4] or CD158 gene complex (7). The inhibitory receptors CD158b1 (or KIR2DL2) and CD158b2 (or KIR2DL3) have ligand specificity for HLA-Cw3 Ags with serine in codon 77 and asparagine in codon 80 of the α1 domain. In contrast, the inhibitory receptor CD158a (or KIR2DL1) has ligand specificity for HLA-Cw4 Ags with asparagine in codon 77 and lysine in codon 80. Accordingly, the CD158a and CD158b inhibitory NK receptors cover the complete spectrum of HLA-Cw Ags identified in the human population. The HLA-Cw Ags and the CD158a/CD158b molecules therefore constitute one receptor-ligand system for tolerance to self (8). Other KIR genes encoding inhibitory receptors with ligand specificity for HLA class I molecules are KIR3DL1 (or CD158e1), recognizing HLA-B molecules containing the Bw4 epitope, and KIR3DL2 (or CD158k), recognizing some HLA-A alleles. In addition, NK cells express other inhibitory receptors for MHC class I molecules. The C-type lectin heterodimer CD94/NKG2A interacts with HLA-E and members of the Ig-like receptor families, Ig-like transcript/leukocyte Ig-like receptor/monocyte-macrophage inhibitory receptor, such as Ig-like transcript 2, which recognize some HLA class I Ags (7). In the absence of inhibitory signals, NK cells are activated by ligand interaction with activating receptors such as natural cytotoxicity receptors, activating KIRs, NKG2D, CD94/NKG2C, 2B4, and others (9, 10).

NK cell-target cell conjugation leads to the formation of an immunological synapse (IS) at the contact site where molecules segregate as activation or inhibition clusters within distinct subdomains of the NKIS (11–14). This dynamic reorganization of molecules have many similarities to the IS described for T cells interacting with APCs (15–19). NK cells form two distinctly different IS, the inhibitory NKIS and the cytolytic NKIS (20).

Temporal and spatial segregation of receptor molecules and other membrane-associated structures into distinct areas of the IS

*Department of Pediatrics and †Immunology Program, Sloan-Kettering Institute for Cancer Research, Memorial Sloan-Kettering Cancer Center, New York, NY 10021

Received for publication January 15, 2004. Accepted for publication May 18, 2004.

The costs of publication of this article were defrayed in part by the payment of page charges. This article must therefore be hereby marked *advertisement* in accordance with 18 U.S.C. Section 1734 solely to indicate this fact.

[1] This work was supported by National Institutes of Health Grants NIAID-K08AI51402 (from National Institute of Allergy and Infectious Diseases; to Y.M.V.), RO1AI50193 (to B.D.), CA08748 (from the National Cancer Institute; MSKCC), and CA59350 (to M.S.); a Junior Faculty Scholar Award from the American Society of Hematology (to Y.M.V.); and the Immune Deficiency Foundation, USA (to Y.M.V.).

[2] Y.M.V. and H.M. contributed equally to this paper.

[3] Address correspondence and reprint requests to Dr. Bo Dupont, Box 41, Memorial Sloan-Kettering Cancer Center, 1275 York Avenue, New York, NY 10021. E-mail address: b-dupont@ski.mskcc.org

[4] Abbreviations used in this paper: KIR, killer cell Ig-like receptor; BLCL, B lymphoblastoid cell line; cSMAC, central SMAC; cSMIC, central SMIC; CTx, cholera toxin β subunit; 2D, two-dimensional; 3D, three-dimensional; EGFP, enriched GFP; MβCD, methyl-β-cyclodextrin; MTOC, microtubule-organizing center; NKIS, NK cell immune synapse; pSMAC, peripheral SMAC; pSMIC, peripheral SMIC; SHP-1, Src homology domain 2-containing PTP-1; SMAC, supramolecular activation cluster; SMIC, supramolecular inhibitory cluster.

0022-1767/04/$02.00

provides a structural framework for regulation of NK cell function. The plasma membrane has specialized cholesterol- and GM1-containing subdomains known as lipid rafts or glycolipid-enriched microdomains. Rafts, which are also important for TCR- and BCR-mediated signaling (21, 22), polarize to the NK-target cell contact site during cytolytic interactions (13, 23). Many signaling molecules become recruited to the rafts, which are constitutively enriched in palmitoylated molecules such as linker for activation of T cells and the Src kinase, Lck (24–26). In contrast, the membrane-associated fractions of Src homology domain 2-containing protein tyrosine phosphatase 1 (SHP-1) are excluded from the rafts. Furthermore, targeting of SHP-1 to rafts profoundly inhibits TCR-mediated activation (27). All inhibitory NK receptors mediate their inhibitory function by recruitment and activation of cytoplasmic tyrosine phosphatases to the ITIM motif within the cytoplasmic domain of the receptor (10, 28, 29), and inhibitory receptors accumulate in the contact area with target cells (11, 30).

It has recently been shown that cognate ligand binding is sufficient to induce clustering of inhibitory KIR and phosphorylation of both the receptor and the phosphatase SHP-1. These events are not dependent on ICAM-1/LFA-1-mediated adhesion and actin polymerization, but require Zn^{2+} and Src kinase activity (31). Signaling-incompetent inhibitory KIR maintain the ability to induce clustering of cognate HLA ligand at the contact site, but do not inhibit raft polarization (13) or actin polymerization (11).

Recruitment and activation of SHP-1 and SHP-2 by a signaling-competent inhibitory receptor are essential early events for initiation of the inhibitory signaling pathways (32–34). This results in inhibition of a multitude of downstream processes, including inhibition of raft polarization and aggregation in the central supramolecular activation cluster (cSMAC), F-actin polymerization, and rearrangement of actin cytoskeleton with translocation of microtubule-organizing center (MTOC) to the area of target cell contact. Up-regulation of LFA-1-mediated cell adhesion and induction of NK effector functions are also inhibited.

It has previously been demonstrated that the location of SHP-1 within the NKIS, as early as 1 min into conjugation, discriminates cytolytic from noncytolytic NK cell interactions with target cells. SHP-1, at this early time point, aggregates in the peripheral supramolecular activation cluster (pSMAC) in cytolytic conjugates, whereas in the noncytolytic conjugates, SHP-1 clusters in the central supramolecular inhibition cluster (cSMIC) (14). Other studies have shown that a mature cytolytic immune synapse is formed with a peripheral talin collar surrounding a central zone that is compartmentalized into one area where granule exocytosis occurs and another where the signaling molecules are concentrated (17, 18). Furthermore, analysis of the IS between T cell and APC indicates that the cSMAC serves the function of enhancing receptor triggering and receptor degradation. This results in an intense, but self-limiting, activation (19). We therefore hypothesized that NK interactions with a susceptible target cell would form a cytolytic IS that would rapidly accumulate signaling molecules and clustered rafts in the cSMAC. During inhibitory interactions we would expect the inhibitory receptors to segregate in the cSMIC and form a platform for recruitment and accumulation of the phosphatases SHP-1 and SHP-2.

We have in the present study used three-dimensional (3D) immunofluorescence microscopy to quantitatively analyze distribution of inhibitory KIR, SHP-1, LFA-1, and lipid rafts within the NKIS during cytolytic and noncytolytic interactions. Human NK clones retrovirally transduced with the inhibitory KIR2DL3 gene fused to GFP were applied. Our analysis demonstrates colocalization of the inhibitory KIR with SHP-1 in the center of inhibitory NKIS. This finding is consistent with the hypothesis that the movement of the receptor into the central area of the IS dictates the inhibitory outcome by providing the activated phosphatase in the environment where concomitant activation signals are building up. Our results also support the hypothesis that the outcome of NK cell-target cell interactions is controlled by quantitative differences in cumulative activating and inhibitory signals.

Materials and Methods

Cells

NK cell clones were generated and maintained from freshly isolated PBMC of healthy donors homozygous for HLA-Cw*0304 as previously described (12, 14). $CD56^+$ $CD3^-$ $GL183^-$ $EB6^-$ $DX9^-$ $CD94^+$ NK clones were used for retroviral infection with KIR2DL3-GFP fusion protein. 2DL3-GFP-transduced and untransduced NK clones were used for conjugation assays with target cells such as 721.221 (class I-negative EBV-BLCL), 721.221-Cw*0401 (non-self allele transfectant), or 721.221-Cw*0304 cells (self allele transfectant) as previously described (12, 14).

Retroviral infection of primary NK cells

DNA encoding KIR2DL3 and enriched GFP (EGFP) was amplified using PCR and subcloned into *Nco*I and *Bam*HI sites of a variant of the pSFG vector. This vector contains the myeloproliferative sarcoma virus long terminal repeat (35). The KIR2DL3-EGFP fusion gene was constructed with EGFP fused at the C terminus cytoplasmic domain of KIR2DL3. KIR2DL3 was amplified by PCR using the forward N-terminal primer 5′-ACGAC CATGGCGCTCATGGTC containing the *Nco*I site and at the reverse C terminal primer 3′-ACGGGATCCGGGCTCAGCATT containing the *Bam*HI site, respectively. The fragment was cleaved and inserted in the pSFG vector at the *Nco*I and *Bam*HI site. This plasmid was sequenced and again cut with *Bam*HI enzyme. EGFP was amplified with the forward N-terminal primer 5′-ACGGGATCCTACCACTCGTT with the *Bam*HI site and with the reverse C-terminal primer 3′-ACGTGGATCCCTACTT GTACAGCTC containing stop codon and the *Bam*HI site. This fragment was then inserted at the *Bam*HI site of the pSFG vector with the KIR2DL3 gene. The plasmid was sequenced to check the orientation of EGFP. This KIR2DL3-EGFP fusion gene containing pSFG plasmid DNA was transfected into the H29 packaging cell line using the calcium phosphate method as previously described (36). Vesicular stomatitis virus G protein pseudotyped retroviral particles were used to infect the PG13 packaging cell line, creating high titer recombinant amphotropic virons pseudotyped with the gibbon ape leukemia virus envelope (37). The virus supernatants were used to infect NK cell clones in the presence of retronectin (Takara, Shuzo, Japan). The plates were coated with retronectin (10 μg/ml) for 2 h at room temperature (36). Viral supernatants were added to the NK cell clones growing in retronectin-coated plates. The transduction efficiency was 5–20%. Both KIR2DL3-EGFP-transduced and untransduced cells were used for conjugation assays.

Antibodies

Primary. NK cells were phenotyped with anti-KIR3DL1 (DX9), anti-KIR2DL3/2DL2/2DS2/2DS3 (GL183), anti-KIR2DL1/2DS1 (EB6), and anti-human CD94 mAbs (Immunotech, Marseilles, France). Anti-CD56 and anti-CD3 were purchased from BD Biosciences (San Jose, CA). The anti-HLA class I mAb, DX17 (IgG1), was a gift from Dr. J. Phillips (DNAX Research Institute, Palo Alto, CA). Mouse monoclonal anti-human talin was purchased from Chemicon International (Temecula, CA), and rabbit polyclonal anti-human SHP-1 and Syk were obtained from Santa Cruz Biotechnology (Santa Cruz, CA). Mouse anti-human lysosome-associated membrane protein (H4A3) and LFA-1 Abs were obtained from the Developmental Studies Hybridoma Bank, University of Iowa (Ames, IA). Mouse monoclonal anti-human α-tubulin (identifies tubules and MTOC) was purchased from Amersham Biosciences (Piscataway, NJ). TRITC-conjugated cholera toxin β subunit (CTx; List Biological Laboratories, Campbell, CA) was used to label lipid raft ganglioside GM1. Primary Abs were titrated for optimal imaging as previously described (14). TRITC-CTx was titrated to optimize staining of NK cells, and a dilution of 1/50, which predominantly stained the NK cell rafts, but not the B cell rafts, was used in the experiments. At a 1/50 dilution of TRITC-CTx, eight of 10 NK-target cell conjugates demonstrated staining only of the NK cell rafts, and only those conjugates with minimal to no staining of the target cell rafts were included in the analysis.

Secondary. Affinity-purified second Abs and species-absorbed conjugates (FITC, Cy3, and Cy5) for multiple labeling were purchased from Chemicon International.

Cholesterol depletion of lipid rafts

For perturbation of rafts, NK cells were treated with different dilutions of methyl-β-cyclodextrin (MβCD; Sigma-Aldrich, St. Louis, MO) in RPMI 1640 medium at 37°C for a period ranging from 5 min to 1 h (38). Treatment of NK cells with 2.5 mM MβCD for 15 min was used for subsequent experiments. At this concentration and duration of treatment, NK cell viability was unaffected (80–85% viable) as determined by trypan blue dye exclusion. Furthermore, NK cell morphology and staining distribution of rafts analyzed by digital immunofluorescence microscopy showed healthy-looking NK cells with typical punctate staining suggestive of adequate cholesterol depletion at this concentration and duration of MβCD treatment. Higher concentrations of MβCD or longer incubation time led to <25% viability and distorted morphology of NK cells.

Conjugation assay and immunofluorescent cell imaging

NK cell-target cell conjugates were immunofluorescently labeled and analyzed after fixing at 1 and 10 min as previously described (12, 14). In all experiments digital imaging system with a Zeiss Axiovert 200M inverted microscope (Intelligent Imaging Innovations, Denver, CO) was used. Images were obtained both in two-dimension (2D; *x*- and *y*-axes) and three-dimension (3D; *x*- and *z*-axes) (12, 14). Quantitative analysis of the entire contact area as well as the peripheral and central subdomains of the contact area was performed using the segmentation and statistics capabilities of SlideBook software (Intelligent Imaging Innovations). Sixty to 70 serial optical sections of 0.2 μm thickness were acquired for each label. The digital recorded data were then deconvolved using Constrained Iterative (3D) Deconvolution algorithm with SlideBook software. The relative enrichment, which is the fluorescence per unit volume at the contact site divided by the fluorescence per unit volume of the entire cell, was calculated for each of the molecules studied as previously described (14). Wilcoxon's nonparametric two-sample test was used to determine the *p* values.

Results

Transduced inhibitory KIR molecules are functional and impart inhibitory specificity for NK cells interacting with target bearing the cognate HLA ligand

The role of the inhibitory KIR2DL3 (2DL3) receptor in the formation and maintenance of NKIS was studied in well-characterized human NK clones, which were retrovirally transduced with 2DL3-GFP fusion construct. Approximately 5–20% of NK cells expressed the transduced receptor (Fig. 1*a*, *left panel*). The transduced 2DL3-GFP receptor in the majority of NK cells was located both on the cell surface as well as in the cytoplasm predominantly around the MTOC (Fig. 1*a*, *bottom panel*). Such subcellular distribution has also been observed for other fluorescence-tagged transduced receptors (39). To test the function of 2DL3-GFP receptor, we selected NK clones that constitutively lacked expression of 2DL3, as determined by mAb GL183, but expressed the transduced 2DL3-GFP receptor (Fig. 1*a*, *top right panel*). Both 2DL3-positive and 2DL3-negative clones were tested for in vitro cytotoxicity against target cells lacking HLA class I molecules (721.221), and target cells expressing only the cognate ligand HLA-Cw*0304 (721.221-Cw*0304) in the presence or the absence of anti-HLA class I (mAb DX17) and anti-2DL3 (mAb GL183) Abs. 2DL3-negative clones were cytotoxic to both targets and the cytotoxicity was not affected by either mAbs (Fig. 1*b*, *top panel*). 2DL3-positive clones were inhibited by 721.221-Cw*0304, and the inhibition was reversed by either of the mAbs (Fig. 1*b*, *bottom panel*). The specificity of HLA-Cw molecules in inhibiting 2DL3-positive clones was further demonstrated in imaging studies. In this study a characteristic cytolytic NKIS with a cSMAC containing Syk kinase and lysosomes surrounded by talin in the periphery (pSMAC) was observed for 2DL3-negative NK cell conjugates with either 721.221-Cw*0304 or 721.221-Cw*0401 target cells (Fig. 1*c*, *two top panels*). This molecular configuration in the NKIS, obtained at 10 min of conjugate formation, is characteristic of a cytolytic interaction as previously described (12).

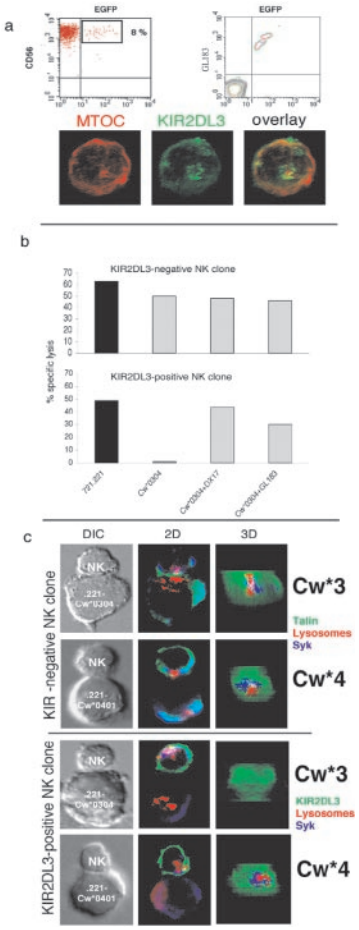

FIGURE 1. Functional reactivity of KIR2DL3-EGFP-transduced NK cells. *a*, Quantitative FACS analysis showing KIR2DL3-EGFP-transduced NK cells (top left) that are constitutively GL183 negative (*top right*). Representative 2D fluorescent image of a KIR2DL3-EGFP-transduced NK cell labeled with α-tubulin to identify MTOC is shown in the overlay (*bottom right*). Either green or red color is removed to better delineate the location of MTOC (*bottom left*) and KIR molecules (*bottom middle*). Note both intracellular and cell surface locations of the transduced KIR. *b*, The cytotoxicity profile of KIR2DL3-negative (*top panel*) and KIR2DL3-positive (*bottom panel*) NK cells against 721.221 (■) and .221-Cw*0304 (▨) target cells in the presence of DX17 or GL183 is shown. *c*, Differential interference contrast (DIC) and fluorescent images (2D and 3D) of KIR-negative (*top two rows*) and KIR2DL3-transduced (*bottom two rows*) NK cell conjugates with .221-Cw*0304 (Cw*3) or .221-Cw*0401(Cw*4) stained with the indicated labels are shown. These conjugates were analyzed 10 min after mixing NK cells with target cells. The data are representative of at least 30 conjugates analyzed for each condition.

When the 2DL3-positive clones were tested with the 721.221-Cw*0304 target cell we observed an inert NKIS at 10 min of conjugate formation. The lysosomes and the Syk kinase did not polarize toward the contact area (2D images), and the contact area had even distribution of 2DL3 molecules (3D image; Fig. 1*c*, *bottom panel*, *top three images*), which is consistent with a mature inhibitory NKIS. In contrast, a cytolytic NKIS was observed only in conjugates between 2DL3-positive clones and the 721.221-Cw*0401 target, which does not express the inhibitory HLA ligand for 2DL3 (Fig. 1*c*, *bottom panel*, *bottom three images*). In this study the lysosomes and Syk were polarized toward the contact area (2D image), and both were located in the cSMAC (3D image). These studies demonstrate that 2DL3-negative NK clones gain inhibitory ligand specificity for Cw*0304 after retroviral transfer of the GFP-tagged 2DL3 receptor.

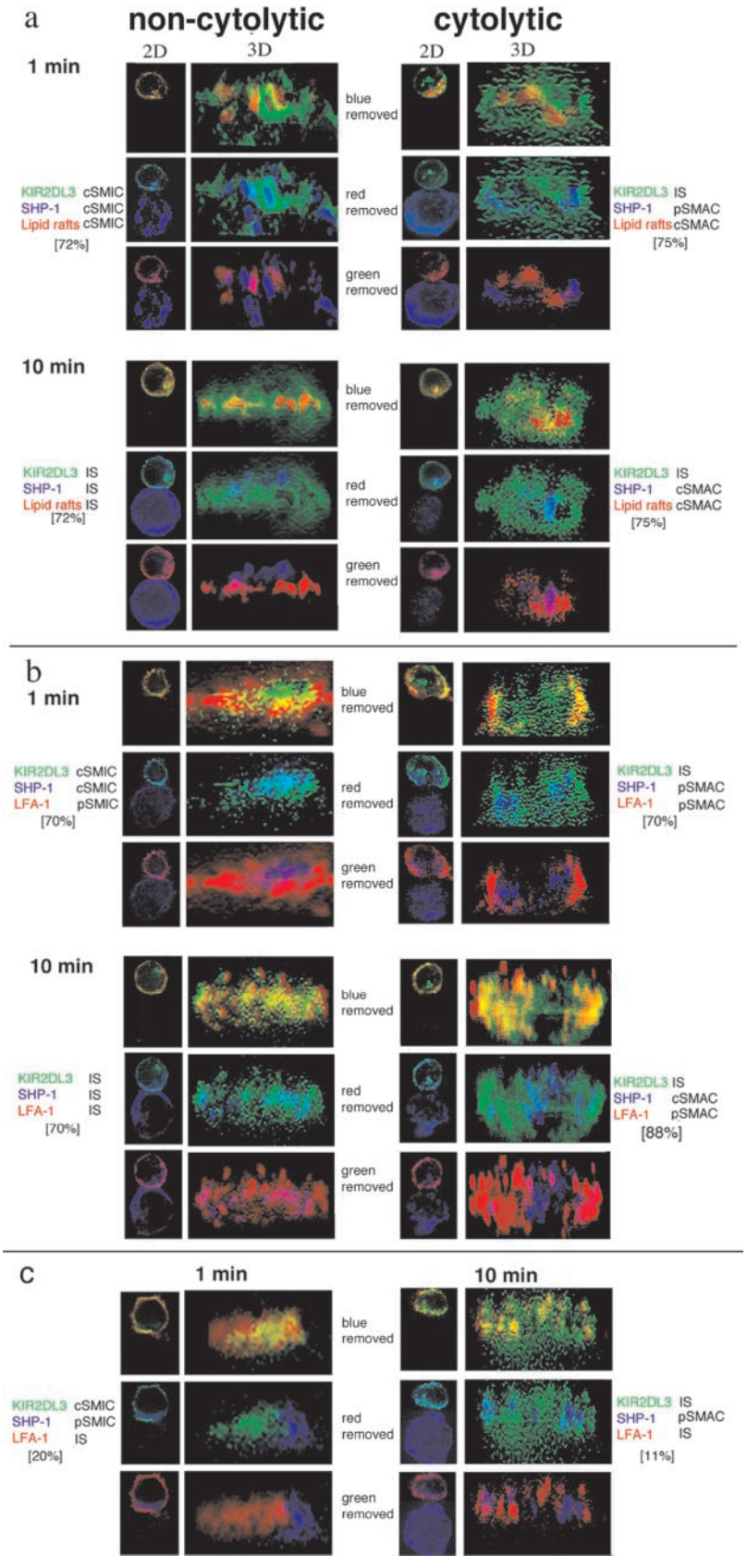

FIGURE 2. Multidimensional temporal-spatial analysis of single NK cell-target cell conjugates. 2D and 3D fluorescent images of KIR2DL3-transduced NK cell conjugates with either .221-Cw*0304 (noncytolytic conjugates; *a–c*) or 721.221 (cytolytic conjugates; *a–c*) stained with the indicated labels and analyzed at 1 and 10 min are shown with blue, red, or green color removed. A representative pattern demonstrated by both a majority (*a* and *b*) and a minority (*c*) of conjugates analyzed at the two time points is shown along with their respective percentages. In all images, the NK cell is the top cell in the conjugate. A description of the location of molecules in the immune synapse (3D images) is shown next to each image. IS, uniform distribution of the molecule within the synapse; c, predominantly central accumulation within the synapse; p, predominantly peripheral accumulation within the synapse. Data in the figure are representative of 30–50 NKIS analyzed.

Location of 2DL3, SHP-1, and rafts in the early and mature inhibitory and cytolytic NKIS

Inhibitory and cytolytic NK cell conjugates were analyzed at 1 min (i.e., early conjugates) and 10 min (i.e., mature conjugates) after mixing with the target cells (Fig. 2). Analysis included localization in the NKIS of 2DL3-GFP, rafts, SHP-1, and LFA-1.

Inhibitory NKIS. The majority of early inhibitory NKIS demonstrates accumulation of 2DL3 in the cSMIC along with a fraction

Table I. *Quantitation of the molecular enrichment within the early and mature cytolytic and noncytolytic immune synapses*[a]

	Noncytolytic Conjugates (Target:.221-Cw*0304)								Cytolytic Conjugates (Target: 721.221)							
	1 min			10 min					1 min			10 min				
				(Majority conjugates)			(Minority conjugates)									
	IS	pSMIC	cSMIC	IS	pSMIC	cSMIC	IS	pSMIC	cSMIC	IS	pSMAC	cSMAC	IS	pSMAC	cSMAC
KIR2DL3	1.15 ± 0.02	1.05 ± 0.02	1.27 ± 0.04	1.03 ± 0.03	0.9 ± 0.02	1.06 ± 0.02	1.18 ± 0.02	1.13 ± 0.01	1.23 ± 0.03	1.06 ± 0.03	1.04 ± 0.02	1.0 ± 0.02	1.19 ± 0.02	1.17 ± 0.02	1.18 ± 0.03
	(n = 43)	p = 0.0001		(n = 28)			(n = 18)	p = 0.0008		(n = 38)			(n = 36)		
SHP-1	1.41 ± 0.05	1.19 ± 0.05	1.63 ± 0.07	1.0 ± 0.05	0.9 ± 0.04	1.08 ± 0.04	1.6 ± 0.06	1.35 ± 0.05	1.84 ± 0.08	1.24 ± 0.05	1.28 ± 0.05	1.06 ± 0.05	1.47 ± 0.06	1.29 ± 0.05	1.61 ± 0.06
	(n = 43)	p = 0.0001		(n = 28)			(n = 18)	p = 0.0002		(n = 38)	p = 0.0001		(n = 36)	p = 0.0001	
Lipid rafts	1.19 ± 0.06	1.07 ± 0.06	1.32 ± 0.07	1.02 ± 0.05	1.0 ± 0.03	1.04 ± 0.05	1.25 ± 0.03	1.15 ± 0.02	1.24 ± 0.06	1.19 ± 0.05	1.14 ± 0.04	1.1 ± 0.06	1.31 ± 0.06	1.11 ± 0.05	1.36 ± 0.05
	(n = 11)	p = 0.0033		(n = 10)			(n = 10)			(n = 13)			(n = 12)	p = 0.0037	
LFA-1	1.14 ± 0.05	1.18 ± 0.07	1.04 ± 0.05	1.22 ± 0.05	1.17 ± 0.07	1.16 ± 0.07	1.21 ± 0.02	1.21 ± 0.03	1.22 ± 0.05	1.09 ± 0.05	1.13 ± 0.05	1.03 ± 0.05	1.4 ± 0.04	1.42 ± 0.05	1.17 ± 0.04
	(n = 13)	p = 0.015		(n = 12)			(n = 4)			(n = 13)	p = 0.033		(n = 13)	p = 0.015	

[a] Degree of accumulation of KIR2DL3, SHP-1, rafts, and LFA-1 as determined by relative enrichment (RE) of the molecules within the entire contact area (i.e., IS), peripheral IS (pSMIC/pSMAC), or central IS (cSMIC/cSMAC) are shown for noncytolytic (*upper panel*) and cytolytic conjugates (*lower panel*) analyzed at the indicated time points. Data representing enrichment in the majority and minority of noncytolytic conjugates at 10 min are also shown. RE = 1.0 is the baseline membrane enrichment for the molecule, and RE = 1.60 is 60% additional accumulation above the baseline. The number of IS analyzed is shown against each molecule and condition studied. SEM values are shown in parentheses. Only significant p values, as determined by Wilcoxon nonparametric statistical test, comparing the enrichment of molecules/structures in peripheral or central subdomains of NKIS are shown.

of membrane-associated SHP-1 (Fig. 2, *a* and *b*, non-cytolytic NKIS, 1 min). It was demonstrated that SHP-1 in the NK cell was polarized toward the target cell (2D images). Coalesced rafts were seen aggregating in the cSMIC in the vicinity of SHP-1, but the distributions of these two components within the early inhibitory NKIS were nonoverlapping (3D images). Furthermore, at this early time point, LFA-1 rapidly redistributed in the pSMIC enclosing the centrally accumulated 2DL3 and SHP-1 (Fig. 2*b*, noncytolytic NKIS, 1 min). This pattern was observed in ~70% of early inhibitory NKIS. A minority of early inhibitory NKIS (~20%) demonstrated another pattern (Fig. 2*c*, noncytolytic NKIS, 1 min). In this study LFA-1 and 2DL3 were beginning to cluster in cSMIC, whereas SHP-1 was not yet recruited to the center. These conjugates may represent very early interactions that are dominated by target cell adhesion and occur before recruitment and activation of SHP-1.

The specific patterning of KIR and SHP-1 observed at 1 min becomes completely resolved in the majority of inhibitory NKIS at 10 min (Fig. 2, *a* and *b*, noncytolytic images, 10 min), although a minority of inhibitory NKIS showed central clustering of 2DL3, SHP-1, and rafts, indicating the formation of early secondary inhibitory interactions (data not shown).

Cytolytic NKIS. In the majority of early cytolytic NKIS (i.e., 1 min), clustered rafts were located in the cSMAC, whereas SHP-1 and LFA-1 were located in the pSMAC (Fig. 2, *a* and *b*, cytolytic images, 1 min). The characteristic location of SHP-1 in pSMAC of cytolytic NKIS was dramatically different from the central location observed at this early time point in the inhibitory NKIS (14). In the mature cytolytic NKIS (i.e., 10 min), clustered rafts were located in the cSMAC together with SHP-1 enclosed in a ring of LFA-1 (Fig. 2, *a* and *b*, cytolytic images, 10 min). A minority of the 10-min cytolytic NKIS displayed molecular configuration reminiscent of early cytolytic NKIS, suggesting the formation of new conjugates at 10 min (Fig. 2*c*, cytolytic images, 10 min). In these conjugates SHP-1 was located in the pSMAC.

Characteristically, in all early cytolytic NKIS the inhibitory 2DL3 receptors did not exhibit any specific pattern of clustering, but were evenly distributed throughout the synaptic region. In mature cytolytic NKIS, 2DL3 receptors appeared to be cleared from the central subdomain of the NKIS where secretory lysosomes accumulated (Fig. 2, *a* and *b*, cytolytic images).

Images were also obtained and analyzed at 5 min (data not shown). This time point provides data representing a mixture of images characteristic of 1 and 10 min; however, they do not provide significant new insights on the spatial and temporal dynamics within NKIS other than illustrating that NK cells form conjugates with targets in a stochastic sequence.

Quantitative enrichment of 2DL3, SHP-1, rafts, and LFA-1 in the inhibitory and cytolytic NKIS

The degree of accumulation (i.e., relative enrichment) of 2DL3, SHP-1, rafts, and LFA-1 within the central and peripheral subdomains of early and mature cytolytic and inhibitory NKIS was also determined. Enrichment of the molecules was determined for the total contact area (i.e., the immune synapse), the peripheral IS (i.e., pSMAC/pSMIC), and the central IS (i.e., cSMAC/cSMIC; Table I).

Inhibitory NKIS. In the early (1 min) inhibitory NKIS, 2DL3, SHP-1, and rafts were significantly more enriched in the cSMIC than in the pSMIC ($p < 0.003$). Although the degree of enrichment of 2DL3, rafts, and LFA-1 in the total synaptic areas was only slightly higher in the early noncytolytic NKIS compared with baseline distribution, these values did not reach statistical significance ($p > 0.10$). Therefore, enrichment of 2DL3 and rafts in the

cSMIC and that of LFA-1 in the pSMIC suggested rapid redistribution into distinct microcompartments of the IS rather than additional recruitment of these molecules/structures into the evolving IS.

The analysis demonstrates that within 1 min into a noncytolytic interaction, ~27 ± 4% of total inhibitory 2DL3 molecules and 63 ± 7% of the total NK cell SHP-1 were recruited to the center of the inhibitory NKIS. In contrast, the majority of mature (10 min) inhibitory NKIS did not show any additional degree of accumulation within the pSMIC or the cSMIC that was above the baseline for 2DL3, SHP-1, or rafts. LFA-1, which in the early NKIS was enriched only in the pSMIC, was redistributed evenly throughout the IS, with no additional LFA-1 being recruited. In a minority of the late inhibitory NKIS, the degree of accumulation of 2DL3 and SHP-1 was similar to that seen in the early inhibitory NKIS. These noncytolytic conjugates may represent new secondary conjugates formed with NK cells that have recently deconjugated from a previous target cell interaction. The uniform enrichment of both LFA-1 and rafts could reflect prolonged membrane changes that have persisted after initial conjugation with a previous target cell.

Cytolytic NKIS. The quantitative analysis of early cytolytic NKIS demonstrated the lack of additional recruitment or redistribution of 2DL3 within the NKIS. In fact, the degree of accumulation of 2DL3 in the IS, pSMAC, or cSMAC was not statistically different between early vs mature cytolytic NKIS. In contrast, the amounts of LFA-1 and SHP-1 enriched in the pSMAC were significantly higher than those in the cSMAC, whereas rafts, although having begun to accumulate in the IS, did not at this early time show any preferential accumulation in the pSMAC or cSMAC. In contrast, the mature cytolytic conjugates showed dramatic enrichment of SHP-1 and rafts in the cSMAC and of LFA-1 in the pSMAC. Therefore, temporal differences in the location and the degree of accumulation of proteins within the microcompartments of the IS distinguish a cytolytic from an inhibitory NK cell interaction.

Perturbation of rafts impacts upon cytolytic, but not inhibitory, NK cell signaling

To analyze the role of rafts in cytolytic and inhibitory signaling during NK cell-target cell interaction, we analyzed NK cell conjugates with either .221-Cw*0304 cells (i.e., inhibitory interaction) or 721.221 (i.e., cytolytic interaction) in NK cells pretreated with MβCD. The NK cells used in these studies were GL183-positive NK clones that displayed cytotoxicity against 721.221 and were noncytotoxic against 721.221-Cw*0304, as previously described (12, 14). NK conjugates with .221-Cw*0304 were analyzed at 1 min, and conjugates with 721.221 were analyzed at 10 min, because at these time points both SHP-1 and rafts were in the central NKIS during inhibitory and cytolytic interactions, respectively (Fig. 2). At 1 min, SHP-1 polarized to the contact area with .221-Cw*0304 in MβCD-treated NK cells (2D image) and was localized in the cSMIC enclosed by a ring of talin (3D image; Fig. 3*a*, *right panel*), similar to the observations made in NK cells not treated with MβCD (compare Fig. 3*a* and Fig. 2, *a* and *b*). Furthermore, 2DL3-positive, MβCD-treated and untreated NK cells remained noncytolytic against 721.221-Cw*0304 target cells (Fig. 3*b*, *right panel*). At 10 min, the analysis of cytolytic conjugates between MβCD-treated NK cells and 721.221 cells demonstrated lack of polarization of SHP-1 and multifocal aggregation of membrane-bound SHP-1 in the NKIS. This observation was in contrast to untreated NK cell conjugates with 721.221, where SHP-1 was polarized to the synapse at 10 min (2D image) and segregated as a unifocal cluster in the cytolytic NKIS (3D image; compare Fig. 2*a*, cytolytic panel, and Fig. 3*a*, *left panel*). Furthermore, MβCD-treated NK cells became noncytolytic against 721.221 target cells (Fig. 3*b*, *left panel*). These studies suggest that raft clustering is not essential for KIR-mediated inhibition to occur, but is required for NK cell cytolytic responses. Most importantly, the translocation of cytoplasmic SHP-1 to the cSMIC in the inhibitory NKIS occurs in the absence of raft clustering.

Discussion

In this study we demonstrate the movements of the inhibitory NK receptor 2DL3 in the NKIS during NK cell interaction with susceptible target cells lacking cognate ligand for 2DL3 and with target cells expressing the cognate ligand, HLA-Cw*0304. The 2DL3 receptor was visualized in the NKIS by retroviral transduction of KIR-negative NK clones with a fusion gene where GFP was linked to the cytoplasmic tail of 2DL3. NK clones gained ligand specificity for cognate HLA-Cw Ags with asparagine in

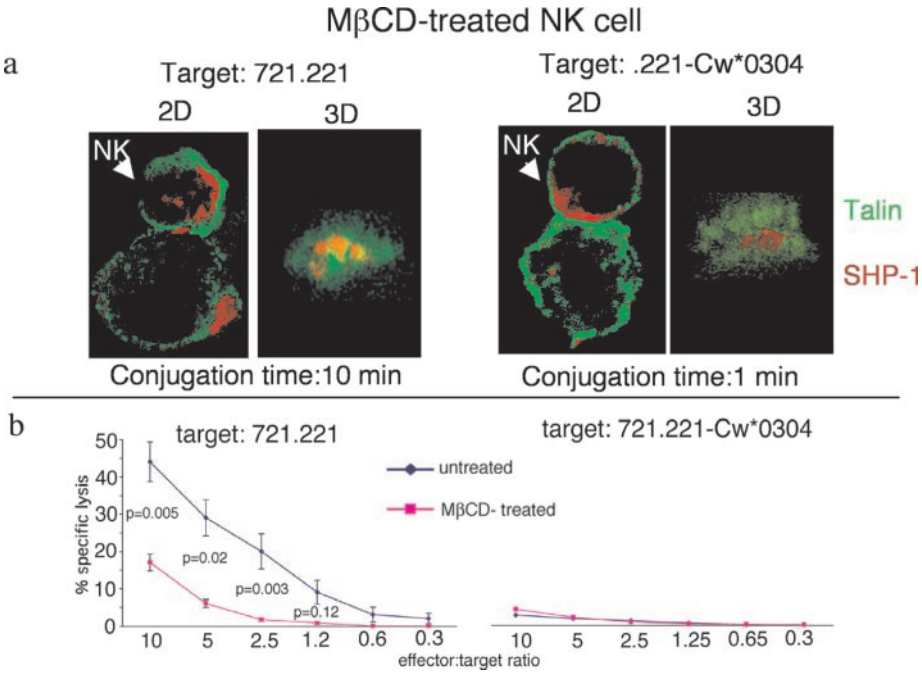

FIGURE 3. The effect of raft perturbation on NK cell function. *a*, 2D and 3D fluorescent images of GL183$^+$ and NKp46$^+$ NK cell conjugates with either 721.221 (*left panel*) or .221-Cw*0304 (*right panel*) dual labeled with indicated molecules (in respective colors) and analyzed at indicated time points is shown. Representative conjugates from NK cells treated with MβCD are shown. The NK cell is the top cell in the conjugates shown in each image. 3D images represent the NKIS visualized as projection in the *x*- and *z*-axes. *b*, Bar graph (±SEM) representing the cytotoxic profile of MβCD-treated and untreated NK cells against 721.221 (*left panel*) and .221-Cw*0304 (*right panel*) is shown for the indicated E:T cell ratio. Data are representative of at least 10–12 NK clones. The *p* values comparing the two cytotoxicity profiles against 721.221 target cells, as determined by Wilcoxon's nonparametric statistical analysis, is shown for each E:T cell ratio.

codon 80, e.g., HLA-Cw*03, whereas NK clones were not inhibited by HLA-Cw ligands with lysine in codon 80, e.g., HLA-Cw*04. We demonstrate by digital immunofluorescence analysis that 2DL3 rapidly accumulates in the center of the inhibitory NKIS during interactions with target cells expressing cognate HLA class I ligand. In contrast, target cells lacking the cognate HLA class I ligand fail to aggregate 2DL3 in any specific subdomains of the cytolytic NKIS. Furthermore, 2DL3 rapidly (within 1 min) colocalizes with SHP-1 in the cSMIC of the inhibitory NKIS. It is also demonstrated that elementary rafts early during the course of the interaction aggregate as clustered rafts in both the cSMIC and cSMAC. The quantitative analysis of relative enrichment demonstrates minimal additional recruitment of rafts into the early inhibitory NKIS from other regions of the NK cell surface. The raft redistribution, i.e., translocation of rafts from the periphery of the synapse into the center, accounts for the enrichment in early inhibitory NKIS, and this finding is consistent with previous studies of Th cell IS (40). In contrast, during cytolytic interactions, recruitment of additional rafts to the mature NKIS does occur. By 10 min of conjugate formation, large clustered rafts are observed in cytolytic NKIS, whereas the inhibitory NKIS at this time point has an inert configuration, except for a few NK cells engaged in formation of new conjugates with other target cells. The observation that aggregation of rafts occurs during the early interactions between NK cell and susceptible target cells as well as with target cells expressing ligands for inhibitory NK receptors demonstrates that early activation signals are also occurring during inhibitory interactions; however, progression into a full-blown cytolytic response is prevented by the early recruitment and activation of SHP-1 into the cSMIC. We also observe rapid formation of a peripheral ring of LFA-1 in pSMIC and pSMAC. This recruitment of LFA-1 becomes further enhanced only during cytolytic interactions, but remains at a low level throughout inhibitory interactions. These findings support the concept that early activation signals during inhibitory interactions are rapidly interrupted and never reach the levels required for strong adhesive binding between LFA-1 and ICAM-1. The quantitative analysis of relative enrichments of fluorescence confirms the impressions gained from visual inspection of the inhibitory and cytolytic NKIS. It is evident that the differential location of SHP-1 at 1 min of conjugate formation clearly defines the subsequent outcome of the NK cell-target cell interactions. The present studies also suggests that the inhibition of NK cytotoxicity induced by inhibitory KIR interactions with cognate ligand may not be caused by translocation of SHP-1 into rafts, as MβCD-mediated raft perturbation did not lift the KIR-HLA inhibition. Although targeting of SHP-1 into rafts does inhibit CD3-induced activation in T cells (27), SHP-1, as shown in this study, is located in the cSMIC during the inhibitory interaction even when raft function is perturbed.

Therefore, early during noncytolytic interaction, the inhibitory receptor recruits SHP-1 into cSMIC and provides a scaffold for the active phosphatases in the central synaptic region where the activation complexes are beginning to accumulate. Rapid recruitment of SHP-1 results in deactivation of these complexes. In contrast, during early cytolytic interaction, SHP-1 is removed from the center of the NKIS and is only brought into the cSMAC at a later time point, thus allowing activation signals to propagate. The recruitment of SHP-1 into the cSMAC of the mature cytolytic NKIS has previously been reported (12) and is consistent with previous studies of the Th cell IS (41). These findings suggest that the location of the cytoplasmic phosphatases within the central microcompartment of the IS plays important roles in terminating activation signals and facilitating receptor recycling also in the NK cells (19, 42). Taken together, our studies support recent findings indicating that NK cells, in contrast to Ag-specific CTL, undergo a series of checkpoints and gradual maturation steps before progression into cytolytic activity (43, 44). Such a requirement by NK cells for stepwise accumulation of activation signals and structural reorganization of the synapse would provide a window for inhibitory receptors in the presence of cognate ligand on the target to exert their function and provide protection against autoreactivity.

Our findings do not support the hypothesis that the inhibitory NKIS has a configuration that is dramatically different from the TCR/MHC-peptide IS. One earlier study indicated that LFA-1 was located in the center of the NKIS surrounded by inhibitory KIR/MHC class I, but these images were obtained at 20 min, which is a late time point where most of the NK cell-target cell interactions and associated signaling have been completed (11). We did, however, identify a minority of inhibitory conjugates (~20%) at 1 min where LFA-1 was located predominantly in the center of the NKIS. In these conjugates SHP-1 was not yet colocalized with 2DL3. This would suggest the formation of early conjugates dominated by adhesion and formed before recruitment and activation of SHP-1. The differences in the location of LFA-1 and inhibitory KIR within the early and mature inhibitory NKIS observed in the present study and the previous report (11) may be due to differences in the NK effector cells used. Although previous studies applied KIR-transduced tumor cell lines that require LFA-1 and CD28 for activation of the lytic response (45, 46), the present study analyzed primary NK clones propagated in IL-2, which do not depend on CD28-CD80/CD86 for their activation.

The recent finding that early dephosphorylation of Vav1 by SHP-1 is the primary pathway used by inhibitory receptors to block activation of NK cytotoxicity is consistent with our observations (33). These investigators suggested that an early, actin polymerization-independent dephosphorylation of Vav1 by SHP-1 blocks subsequent downstream activation signals. These studies together with the observation that NK cell activation requires multiple, cumulative activation signals, allowing inhibitory signals to terminate the activation signals (43, 44), are in agreement with our findings. NK cell activation, in our model, is dependent upon a sequential series of activation signals that occur when target cells lack ligands for inhibitory receptors. Raft aggregation depends upon protein kinase C-θ translocation and Vav1/Rac-induced actin-cytoskeleton reorganization (47, 48). In the presence of such ligands, activating signals are interrupted as long as the inhibitory signals are provided within the allowed finite time frame. Recent studies have demonstrated that cognate ligand for inhibitory KIRs expressed on insect cells can induce clustering of KIR and phosphorylation of KIR and SHP-1 (31). These studies did not address the concomitant signals provided by other receptor-ligand interactions occurring under more physiological conditions. Although ligand binding to inhibitory receptor is capable of inducing receptor phosphorylation and phosphatase recruitment and activation, there are concomitant activation signals that also contribute to these events. Due to the prolonged time required by NK cells to be activated relative to Ag-specific CTLs, all these activation signals are therefore interrupted, and NK cell activation does not occur when the cumulative activation signals fail to exceed the threshold defined by the sum of the inhibitory signals. Addition of activation signals provided by ligand binding to activating receptors such as NKG2D or natural cytotoxicity receptor (i.e., natural cytotoxicity receptors NKp46, NKp44, and NKp30) may override this inhibition (10, 49). The mechanism by which such additional signals change the balance between activation and inhibition and how this affects the formation of NKIS are currently under investigation.

Acknowledgments

We thank Dr. J. Phillips (DNAX Research Institute, Palo Alto, CA) for anti-HLA class I mAb DX17, and Dr. Peter Parham (Stanford University, Palo Alto, CA) for BLCL 721.221+Cw*0304 and 721.221+Cw*0401 and Dr. Lloyd J. Old (Ludwig Institute for Cancer Research, New York Branch) for access to digital fluorescence microscope with SlideBook software.

References

1. Biron, C. A., K. B. Nguyen, G. C. Pien, L. P. Cousens, and T. P. Salazar-Mather. 1999. Natural killer cells in antiviral defense: function and regulation by innate cytokines. *Annu. Rev. Immunol. 17:189.*
2. Ljunggren, H. G., and K. Karre. 1990. In search of the 'missing self:' MHC molecules and NK cell recognition. *Immunol. Today 11:237.*
3. Bauer, S., V. Groh, J. Wu, A. Steinle, J. H. Phillips, L. L. Lanier, and T. Spies. 1999. Activation of NK cells and T cells by NKG2D, a receptor for stress-inducible MICA. *Science 285:727.*
4. Cosman, D., J. Mullberg, C. L. Sutherland, W. Chin, R. Armitage, W. Fanslow, M. Kubin, and N. J. Chalupny. 2001. ULBPs, novel MHC class I-related molecules, bind to CMV glycoprotein UL16 and stimulate NK cytotoxicity through the NKG2D receptor. *Immunity 14:123.*
5. Diefenbach, A., A. M. Jamieson, S. D. Liu, N. Shastri, and D. H. Raulet. 2000. Ligands for the murine NKG2D receptor: expression by tumor cells and activation of NK cells and macrophages. *Nat. Immunol. 1:119.*
6. Cerwenka, A., A. B. Bakker, T. McClanahan, J. Wagner, J. Wu, J. H. Phillips, and L. L. Lanier. 2000. Retinoic acid early inducible genes define a ligand family for the activating NKG2D receptor in mice. *Immunity 12:721.*
7. Vilches, C., and P. Parham. 2002. KIR: diverse, rapidly evolving receptors of innate and adaptive immunity. *Annu. Rev. Immunol. 20:217.*
8. Arase, H., E. S. Mocarski, A. E. Campbell, A. B. Hill, and L. L. Lanier. 2002. Direct recognition of cytomegalovirus by activating and inhibitory NK cell receptors. *Science 296:1323.*
9. Moretta, A., C. Bottino, M. Vitale, D. Pende, C. Cantoni, M. C. Mingari, R. Biassoni, and L. Moretta. 2001. Activating receptors and coreceptors involved in human natural killer cell-mediated cytolysis. *Annu. Rev. Immunol. 19:197.*
10. Lanier, L. L. 2003. Natural killer cell receptor signaling. *Curr. Opin. Immunol. 15:308.*
11. Davis, D. M., I. Chiu, M. Fassett, G. B. Cohen, O. Mandelboim, and J. L. Strominger. 1999. The human natural killer cell immune synapse. *Proc. Natl. Acad. Sci. USA 96:15062.*
12. Vyas, Y. M., K. M. Mehta, M. Morgan, H. Maniar, L. Butros, S. Jung, J. K. Burkhardt, and B. Dupont. 2001. Spatial organization of signal transduction molecules in the NK cell immune synapses during MHC class I-regulated noncytolytic and cytolytic interactions. *J. Immunol. 167:4358.*
13. Fassett, M. S., D. M. Davis, M. M. Valter, G. B. Cohen, and J. L. Strominger. 2001. Signaling at the inhibitory natural killer cell immune synapse regulates lipid raft polarization but not class I MHC clustering. *Proc. Natl. Acad. Sci. USA 98:14547.*
14. Vyas, Y. M., H. Maniar, and B. Dupont. 2002. Cutting edge: differential segregation of the SRC homology 2-containing protein tyrosine phosphatase-1 within the early NK cell immune synapse distinguishes noncytolytic from cytolytic interactions. *J. Immunol. 168:3150.*
15. Monks, C. R., B. A. Freiberg, H. Kupfer, N. Sciaky, and A. Kupfer. 1998. Three-dimensional segregation of supramolecular activation clusters in T cells. *Nature 395:82.*
16. Potter, T. A., K. Grebe, B. Freiberg, and A. Kupfer. 2001. Formation of supramolecular activation clusters on fresh ex vivo $CD8^+$ T cells after engagement of the T cell antigen receptor and CD8 by antigen-presenting cells. *Proc. Natl. Acad. Sci. USA 98:12624.*
17. Stinchcombe, J. C., G. Bossi, S. Booth, and G. M. Griffiths. 2001. The immunological synapse of CTL contains a secretory domain and membrane bridges. *Immunity 15:751.*
18. Kuhn, J. R., and M. Poenie. 2002. Dynamic polarization of the microtubule cytoskeleton during CTL-mediated killing. *Immunity 16:111.*
19. Lee, K. H., A. R. Dinner, C. Tu, G. Campi, S. Raychaudhuri, R. Varma, T. N. Sims, W. R. Burack, H. Wu, J. Wang, et al. 2003. The immunological synapse balances T cell receptor signaling and degradation. *Science 302:1218.*
20. Vyas, Y. M., H. Maniar, and B. Dupont. 2002. Visualization of signaling pathways and cortical cytoskeleton in cytolytic and noncytolytic natural killer cell immune synapses. *Immunol. Rev. 189:161.*
21. Dykstra, M., A. Cherukuri, H. W. Sohn, S. J. Tzeng, and S. K. Pierce. 2003. Location is everything: lipid rafts and immune cell signaling. *Annu. Rev. Immunol. 21:457.*
22. Xavier, R., T. Brennan, Q. Li, C. McCormack, and B. Seed. 1998. Membrane compartmentation is required for efficient T cell activation. *Immunity 8:723.*
23. Lou, Z., D. Jevremovic, D. D. Billadeau, and P. J. Leibson. 2000. A balance between positive and negative signals in cytotoxic lymphocytes regulates the polarization of lipid rafts during the development of cell-mediated killing. *J. Exp. Med. 191:347.*
24. Parolini, I., S. Topa, M. Sorice, A. Pace, P. Ceddia, E. Montesoro, A. Pavan, M. P. Lisanti, C. Peschle, and M. Sargiacomo. 1999. Phorbol ester-induced disruption of the CD4-Lck complex occurs within a detergent-resistant microdomain of the plasma membrane. Involvement of the translocation of activated protein kinase C isoforms. *J. Biol. Chem. 274:14176.*
25. Zhang, W., R. P. Trible, and L. E. Samelson. 1998. LAT palmitoylation: its essential role in membrane microdomain targeting and tyrosine phosphorylation during T cell activation. *Immunity 9:239.*
26. Inoue, H., M. Miyaji, A. Kosugi, M. Nagafuku, T. Okazaki, T. Mimori, R. Amakawa, S. Fukuhara, N. Domae, E. T. Bloom, et al. 2002. Lipid rafts as the signaling scaffold for NK cell activation: tyrosine phosphorylation and association of LAT with phosphatidylinositol 3-kinase and phospholipase C-γ following CD2 stimulation. *Eur. J. Immunol. 32:2188.*
27. Su, M. W., C. L. Yu, S. J. Burakoff, and Y. J. Jin. 2001. Targeting Src homology 2 domain-containing tyrosine phosphatase (SHP-1) into lipid rafts inhibits CD3-induced T cell activation. *J. Immunol. 166:3975.*
28. Burshtyn, D. N., A. M. Scharenberg, N. Wagtmann, S. Rajagopalan, K. Berrada, T. Yi, J. P. Kinet, and E. O. Long. 1996. Recruitment of tyrosine phosphatase HCP by the killer cell inhibitor receptor. *Immunity 4:77.*
29. Ravetch, J. V., and L. L. Lanier. 2000. Immune inhibitory receptors. *Science 290:84.*
30. Eriksson, M., J. C., Ryan, M. C. Nakamura, and C. L. Sentman. 1999. Ly49A inhibitory receptors redistribute on natural killer cells during target cell interaction. *Immunology 97:341.*
31. Faure, M., D. F. Barber, S. M. Takahashi, T. Jin, and E. O. Long. 2003. Spontaneous clustering and tyrosine phosphorylation of NK cell inhibitory receptor induced by ligand binding. *J. Immunol. 170:6107.*
32. Yusa, S.-I., and K. S. Campbell. 2003. Src homology region 2-containing protein tyrosine phosphatase-2 (SHP-2) can play a direct role in the inhibitory function of killer cell Ig-like receptors in human NK cells. *J. Immunol. 170:4539.*
33. Stebbins, C. C., C. Watzl, D. D. Billadeau, P. J. Leibson, D. N. Burshtyn, and E. O. Long. 2003. Vav1 dephosphorylation by the tyrosine phosphatase SHP-1 as a mechanism for inhibition of cellular cytotoxicity. *Mol. Cell. Biol. 23:6291.*
34. Zhenkun, L., D. D. Billadeau, D. N. Savoy, R. A. Schoon, and P. J. Leibson. 2001. A role for a RhoA/ROCK/LIM-kinase pathway in the regulation of cytotoxic lymphocytes. *J. Immunol. 167:5749.*
35. Ericikan-Abali, E. A., S. Mineishi, Y. Tong, S. Nakahara, M.C. Waltham, D. Banerjee, W. Chen, M. Sadelain, and J. R. Bertino. 1996. Active site directed double mutants of dihydrofolate reductase. *Cancer Res. 56:4142.*
36. Riviere, I., and M. Sadelain. 1997. Methods for the construction of retroviral vectors and the generation of high titer producers. In: *Methods in Molecular Medicine, Gene Therapy Protocols*. P. Robbins, ed. Humana Press, Clifton, p. 59.
37. Miller, A. D., J. V. Garcia, N. Von Suhr, C. M. Lynch, C. Wilson, and M. V. Eiden. 1991. Construction and properties of retrovirus packaging cells based on gibbon ape leukemia virus. *J. Virol. 65:2220.*
38. Lindwasser, O. W., and M. D. Resh. 2002. Myristoylation as a target for inhibiting HIV assembly: unsaturated fatty acids block viral budding. *Proc. Natl. Acad. Sci. USA 99:13037.*
39. Zal T, M. A. Zal, and N. R. Gascoigne. 2002. Inhibition of T cell receptor-coreceptor interactions by antagonist ligands visualized by live FRET imaging of the T-hybridoma immunological synapse. *Immunity 16:521.*
40. Burack, W. R., K.-H. Lee, A. D. Holdorf, M. L. Dustin, and A. S. Shaw. 2002. Cutting edge: quantitative imaging of raft accumulation in the immunological synapse. *J. Immunol. 169:2837.*
41. Kosugi, A., J. Sakakura, K. Yasuda, M. Ogata, and T. Hamaoka. 2001. Involvement of SHP-1 tyrosine phosphatase in TCR-mediated signaling pathways in lipid rafts. *Immunity 14:669.*
42. Huppa, J. B., and M. M. Davis. 2003. T-cell-antigen recognition and the immunological synapse. *Nat. Rev. 3:973.*
43. Wülfing, C., B. Purtic, J. Klem, and J. D. Schatzle. 2003. Stepwise cytoskeletal polarization as a series of checkpoints in innate but not adaptive cytolytic killing. *Proc. Natl. Acad. Sci. USA 100:7767.*
44. Orange, J. S., K. E. Harris, M. M. Andzelm, M. M. Valter, R. S. Geha, and J. L. Strominger. 2003. The mature activating natural killer cell immunologic synapse is formed in distinct stages. *Proc. Natl. Acad. Sci. USA 100:14151.*
45. Asuma, M., M. Cayabyab, D. Buck, J. H. Phillips, and L. L. Lanier. 1992. Involvement of CD28 in MHC-unrestricted cytotoxicity mediated by a human natural killer leukemia cell line. *J. Immunol. 149:1115.*
46. Teng, J. M., X. R. Liu, G. B. Mills, and B. Dupont. 1996. CD28-mediated cytotoxicity by the human leukemic NK cell line YT involves tyrosine phosphorylation, activation of phosphatidylinositol 3-kinase, and protein kinase C. *J. Immunol. 156:3222.*
47. Villalba, M., K. Bi, F. Rodriguez, Y. Tanaka, S. Schoenberger, and A. Altman. 2001. Vav1/Rac-dependent actin cytoskeleton reorganization is required for lipid raft clustering in T cells. *J. Cell Biol. 155:331.*
48. Bi, K., Y. Tanaka, N. Coudronniere, K. Sugie, S. Hong, M. J. B. van Stipdonk, and A. Altman. 2001. Antigen-induced translocation of PKC-θ to membrane rafts is required for T cell activation. *Nature 2:556.*
49. Diefenbach, A., and D. H. Raulet. 2002. The innate immune response to tumors and its role in the induction of T-cell immunity. *Immunol. Rev. 188:9.*